Effect of coating thickness on the tool wear performance of low stress TiAlN PVD coating during turning of compacted graphite iron (CGI)

Majid Abdoos[a,*], Kenji Yamamoto[b], Bipasha Bose[a], German Fox-Rabinovich[a], Stephen Veldhuis[a]

[a] McMaster Manufacturing Research Institute (MMRI), Department of Mechanical Engineering, McMaster University, Hamilton, ON, Canada L8S 4L7
[b] Materials Research Laboratory, Kobe Steel Ltd., Kobe 651-2271, Japan

ABSTRACT

Compacted graphite iron (CGI), with its superior mechanical properties, is a promising candidate to replace grey cast iron in the automotive industry. However, the low machinability of CGI compared to grey cast iron, has made this transition difficult. Built-up edge formation, combined with abrasive and adhesive wear is the main problem of CGI turning at moderate cutting speeds. In this study, a low compressive residual stress PVD coating was developed using newly introduced super fine cathode (SFC) technology. The main advantage of low compressive residual stress SFC coating, is the possibility of increasing its thickness compared to the commercial range of arc coatings (usually with a thickness within 1–5 μm) without any process induced spallation of the coating layer. Therefore, three different low compressive residual stress $Ti_{40}Al_{60}N$ coatings with thicknesses of around 5, 11 and 17 μm were deposited. The coatings were characterized by X-Ray diffraction, scratch test, ball crater test and nanoindentation. Furthermore, the cutting performance of the coated inserts was investigated in finish turning of CGI. An improvement of around 35% tool life is achieved for the cutting tool with the low residual stress thick coating compared to the commercial benchmark. Progression of flank wear was studied by means of TEM, SEM-EDS, optical microscopy and 3D wear measurement. Chip undersurface morphology as well as cross-sectional studies of the chip structure were performed. This was combined with analysis of the work-piece surface. Evaluation of the results obtained would help to achieve a better understanding of the wear mechanism and built-up edge formation of the studied coatings. According to the recorded data, coating thickness significantly affects cutting tool wear behavior and the mechanical properties of the coatings. A certain thickness range, specifically within 10 μm was found to be optimum.

1. Introduction

Compacted graphite iron or CGI is from the cast iron family with its mechanical properties falling between grey cast iron and ductile cast iron. Graphite in CGI is randomly oriented similar to grey cast iron; however, it is thicker in size and has round edges with a unique structure. Unlike ductile cast iron and grey cast iron, CGI has a coral like structure with a bumpy surface that provides strong adhesion between the iron matrix and graphite. Therefore, the superior mechanical properties of CGI make it a potential replacement for grey cast iron in the automotive industry [1,2]. However, CGI has a lower machinability than grey cast iron since tool life variability complicates the transition [3].

It is known that poor machinability of CGI compared to grey cast iron comes from its superior mechanical properties [4] and difference in composition [5]. During machining of grey cast iron, a dense MnS layer forms on the tool, which acts as a lubricant and protects the tool from wear. As the compacted graphite structure is only stable at a low oxygen and sulfur content, no protective layer forms on the tool during machining of CGI, resulting in higher tool wear [6,7]. Lack of lubricating graphite due to its coral-like structure [8], presence of hard abrasive compounds [9] and higher temperature generated during machining [10], further decreases the CGI tool life. All of these factors result in dominant adhesive and abrasive wear of the tool during CGI machining. Diffusion and oxidation wear are also reported in some cases, but their effect on tool life less significant [11,12]. Abrasive wear during machining of CGI is mostly caused by abrasive particles such as titanium or vanadium carbo-nitrides and can be reduced by controlling the chemical composition [9,12]. On the other hand, adhesive wear followed by micro chipping, built-up edge and layer formation is more

dominant at a higher cutting speed and cutting temperature [11]. Lubricating and cooling the cutting zone to achieve a lower temperature, leads to moderate success in reducing the adhesion of CGI [13,14]. Recently, Tooptong et al. [15] explored different coatings to improve the machinability of CGI. It was reported that adhesion can be reduced via proper coating design. However, there exists no in-depth study to substantiate this claim.

PVD coatings are currently being successfully deposited on cutting tools in the thickness of 1–5 μm. To improve tool life, several attempts have been made to increase the thickness beyond 5 μm [16–19]. However, due to limitations of the deposition process provoking high residual stress distribution and strain energy, high thickness coatings are apt to early failure [20]. Tuffy et al. [20] observed that as the thickness of the TiN coating increases beyond 3.5 μm, tool life diminishes due to chipping and cracking at the tool tip caused by high compressive residual stress. Sargade et al. [21] observed similar results for 6.7 μm thick TiN coating and reported early failure due to coating spallation. In another study, Klocke et al. [22] was able to prolong the tool life during turning by increasing the thickness of the TiAlN coating to 8 μm. As the coating thickness increases, a greater volume of material is available to wear out until substrate exposure. Bouzakis et. al [16,17] studied the effect of thickness (2–10 μm) on the mechanical properties and wear resistance of the $Ti_{46}Al_{54}N$ coating. Although an increase in thickness had a negative effect on the mechanical properties of the coating, the tool life was seen to improve in the milling application. In agreement with this study, Skordaris et al. [18] achieved an improvement in tool life by increasing the thickness of the $Ti_{46}Al_{54}N$ PVD coating to 8 μm. The excess residual stress is released through a low deposition rate (1 μm per hour) and therefore the coating was annealed during the deposition. The reported increase in the tool life has two causes: first, the substrate is protected for a longer duration as the thickness increases. Second, as the coating becomes thicker, edge roundness also increases, which reduces stress concentration on the coating.

Previous studies show that thick PVD coatings provide superior thermal and stress protection to the tool and increase its life by delaying substrate exposure [18], thus improving resistance to abrasion and adhesion during the machining of CGI. This paper investigates the effect of coating thickness on edge geometry, mechanical properties of the film, adhesion, tool wear and surface integrity. In this context, 5–20 μm thick multilayered TiAlN coatings were deposited under a low residual stress state using super fine cathode (SFC) technology and their performance was evaluated in finish turning of CGI.

2. Experimental procedure

AlTiN coatings of different thicknesses were produced by a cathodic arc ion plating process using a Kobelco AIP-S20 deposition system. The system uses two SFC (super fine cathode) arc evaporation sources with extended plasma range for the deposition process. SFC is a new technology capable of depositing more than 20 μm thick coatings with low compressive residual stress. The features of this technology were detailed elsewhere [19]. In the current study, coatings of three different thicknesses were deposited on Kennametal ISO CNGG432FS and Sandvik Coromant ISO SPGN120308 polished uncoated inserts using an arc evaporation source produced by powder metallurgy, composed of 40% Ti and 60% Al. Prior to the deposition, substrate inserts were cleaned in acetone with an ultrasonic cleaner, mounted inside the deposition chamber and then heated to 550 °C. Ar etching was done at 1.3 Pa Ar pressure for 7.5 min to increase adhesion and reduce any contamination in the coating. The coatings were produced in a multilayer state using bilayers deposited with bias voltages of − 30 V and − 70 V, thickness of the coating is varied by adjusting the number of bilayers. The deposition parameters are given in Table 1.

For coating characterisation, the thickness is measured with a ball crater system of a 25 mm diameter. Residual stress was measured with a

Table 1
Deposition parameters for SFC deposited coatings.

Bias voltage	Arc source current	Ar-N_2 atmosphere		Rotational speed
		Temperature	Pressure	
− 30 V/ − 70 V	100 A	550 °C	4 Pa	table rotation at 5 rpm

2-dimension X-Ray diffraction (XRD^2) system, Bruker D8 Discover instrument with cobalt radiation and a wavelength of 1.79 Å (K_α). Residual stress was calculated on (220) crystallographic plane using LEPTOS software, details of the process can be found elsewhere [23]. The micromechanical properties of the coating were evaluated on a Micro Materials NanoTest system, and nanoindentation was performed with a load control mode at a load of 100mN. The load was adjusted according to surface roughness of the samples and so that the depth of penetration would be less than 10% of the total thickness to eliminate the substrate effect. A Berkovich diamond indenter was used to perform 40 indents on each coating. To study adhesive and cohesive failure of the coating, scratch test was performed on flat coated inserts with an Anton Paar Revetest scratch tester using a Rockwell C diamond indenter with a 100 μm radius. Scratch parameters are as follows: progressive loading from 0.5 N to 100 N, scratch length of 3 mm and scratching velocity of 7.5 mm/min.

To evaluate performance of the coated tool inserts, a hollow cylindrical shape of the workpiece material (CGI) was used, with an outer diameter of 120 mm, an inner diameter of 80 mm and a length of 200 mm. The workpiece consisted of 70% pearlite with 20% nodularity. CGI turning was performed using an OKUMA CNC Crown L1060 lathe CNC machine. CNGG432FC inserts with an AlTiN KC5010 coating supplied by Kennametal were used as a benchmark to compare the coating performance. The cutting test was conducted for the finishing operation under dry condition with a cutting speed of 300 m/min, feed rate of 0.2 mm/rev and 0.25 mm depth of cut. Flank wear was measured after a certain cutting length with a Keyence VHX-5000 microscope. Edge radius and volumetric difference measurement of the tool was done with an Alicona optical microscope equipped with focus variation technology. The same instrument was used for surface roughness measurement under ISO standards 4287 and 25178. The cutting tests were continued until a maximum flank wear of 300 μm was reached according to ISO 3685 standard. During the cutting process, cutting forces were measured with a 3D component tool holder Kistler dynamometer type 9121. To better understand the wear mechanism, cutting tools were studied at certain cutting lengths using a Vega 3-TESCAN SEM equipped with EDS. FIB (focused ion beam) cross section analysis of the rake face of the tool further investigated the mechanism of wear by transmission electron microscopy (TEM) JEOL FS2200.

3. Results and discussion

To evaluate the machining performance of the coating, basic understanding of its properties is needed. This section characterizes the coating by various methods such as nanoindentation, XRD and the scratch test, followed by an in-depth machining study.

3.1. Coating characterisation

Three different thicknesses of TiAlN coating were successfully deposited using the SFC technology. Optical inspection of the coatings showed no delamination or process-induced damage on the coating. Thickness of the coatings was measured on SPGN120308 flat inserts using a ball crater test, Fig. 1(a) and Table 2 shows the maximum thickness of about 17 μm. It is worth mentioning that higher deposition rate and lower deposition time comparing to literature [18] can be

Table 2
Coating thickness vs. deposition time.

Coating	Total deposition time	Number of bilayer	Thickness (µm)
Benchmark (KC5010)	NA	NA	4.64 ± 0.46
T1	42 min	14	5.38 ± 0.49
T2	84 min	28	11.41 ± 0.48
T3	144 min	42	17.15 ± 0.58

achieved with the aforementioned method as shown in Table 2. Deposition rate decreased with time; however, the change is quite insignificant. Each bilayer deposited with − 30/− 70 bias voltage is approximately 400 nm. All of the coatings are in a compressive residual stress state as seen in Fig. 1(b), T1-T3 coatings are under low residual stress compared to the benchmark. This was expected from the nature of the SFC technology and low bias voltage implementation during the deposition process. Beside affecting the mechanical properties, the increased thickness has a significant effect on tool geometry of the coated inserts. Mean values of edge roundness from 40 measurements along the cutting edge (Fig. 1(c)) show a drastic increase in the edge radius as the coating becomes thicker.

Fig. 2(a) and (b) depicts hardness and elastic modulus of SFC deposited (T1-T3) and benchmark coatings measured by nanoindentation. Increase in the thickness has a minor effect on hardness and elastic modulus values of the coatings and mechanical strength of the coating does not decrease as was previously reported [16]. This decrease in hardness and mechanical strength is mentioned to be due to grain growth corresponding to columnar microstructure and is not observed here due to the multilayer state of the coating. It is also worth mentioning that the coatings deposited by SFC have a higher hardness compared to the commercial coating.

To study cohesive (through the coating) and adhesive (coating/substrate interface) behavior of the coatings, two critical loads were measured during the scratch test: Lc_1, the critical load at which continuous cracking begins and Lc_2, the critical load at which the substrate is exposed. Figs. 2(c) and (d) show that as coating thickness increases, Lc_1 and Lc_2 values shift towards higher loads. Consequently, the failure mode spreads further away from the scratch track until total

delamination and substrate exposure of the T3 coating (Fig. 3). The effect of increasing thickness on greater critical loads and failure damage has been observed by many researchers [24,25] and is believed to be due to the greater normal load required to be present on the surface to induce the same amount of shear stress in the interface [26]. Therefore, the variation of Lc_2 in T1-T3 is believed to be due to the difference in thickness and thus does not reliably indicate adhesion to the substrate for different coatings. However, Lc_1 can be used as a simple estimation of crack resistance [27]. Comparing the different coatings in this way, it can be concluded that SFC deposited coatings with lower compressive residual stress values are more prone to cracking and cohesive failure.

3.2. Machining studies

SFC technology makes it possible to reduce residual stress on the deposited coating and as a result, the coating becomes less resistant to cohesive failure. This factor becomes crucial when adhesive wear is manifested during dry machining of CGI. Therefore, understanding the effect of low residual stress on tool wear is of utmost importance.

3.2.1. Tool life and cutting force

Progression of flank wear with respect to cutting length during CGI finish turning is illustrated in Fig. 4. Benchmark (KC5010) and T1 coatings have an almost identical tool life behavior. As coating thickness increases from T1 to T2, an improvement of around 35% in tool life is achieved. However, further thickness increase causes premature failure after a short length of cut. The premature failure of the T3 coating is strongly related to the change in tool microgeometry caused by increased thickness (Fig. 1(b)). In fact, an increase in edge radius promotes ploughing [28] which in turn increases cutting forces (Fig. 5), lowers stress concentration on the coating, increases heat generation as well as heat dissipation due to greater contact between the tool and workpiece/chip [29]. Consequently, as tool life becomes more affected by it, there emerges an optimum range of cutting edge radii and going out of this range will reduce tool life.

Progression of tool wear is shown in Fig. 6 with 3D difference measurement of the cutting edge. Wear is mostly focused on the cutting edge which indicates that dominant wear is caused by adhesion of CGI
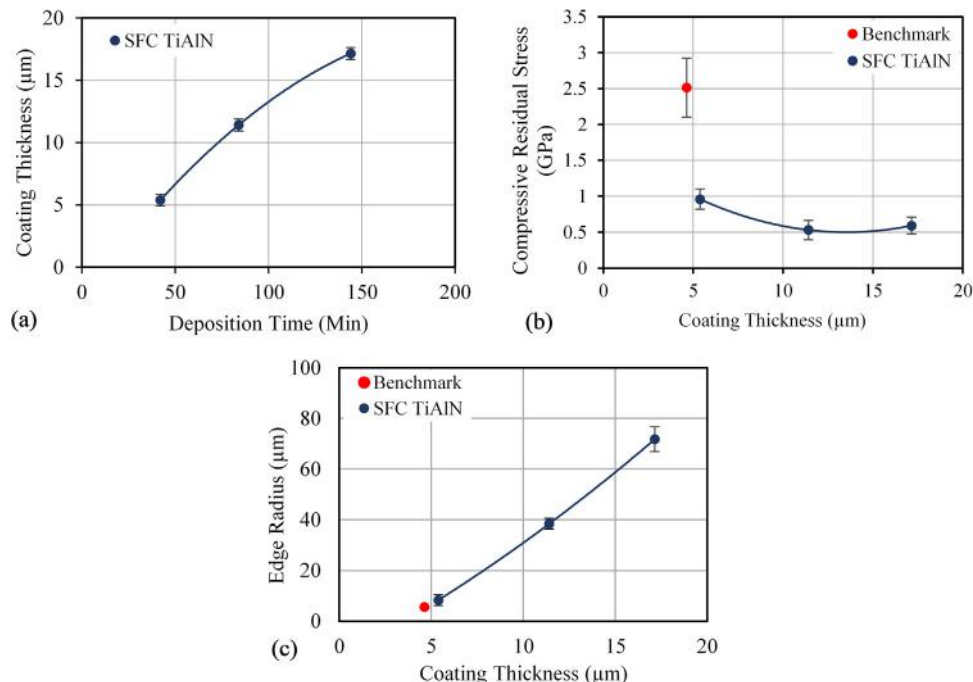
Fig. 1. Effect of deposition time on coating thickness (a), residual stress (b) and edge radius (c) vs. thickness.
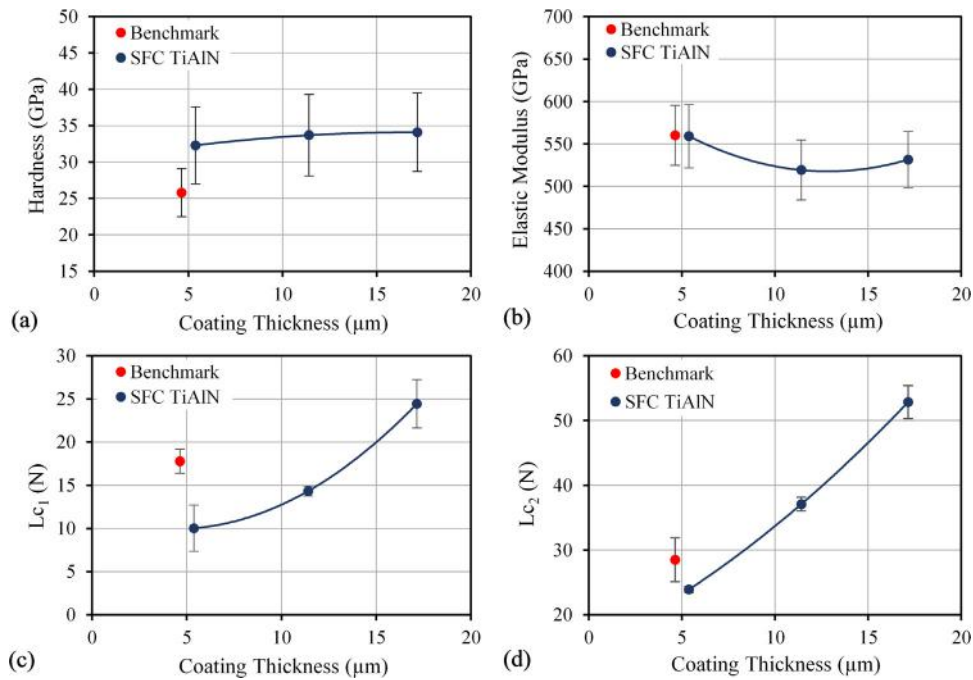
Fig. 2. Variation of properties with coating thickness, Hardness (a), Modulus of Elasticity (b), Lc_1 (c) and Lc_2 (d).
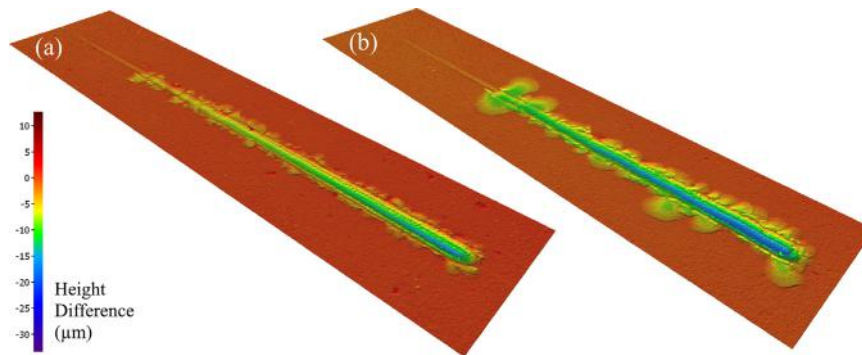
Fig. 3. 3D scratch track map of benchmark (a) and T2 (b) coating.
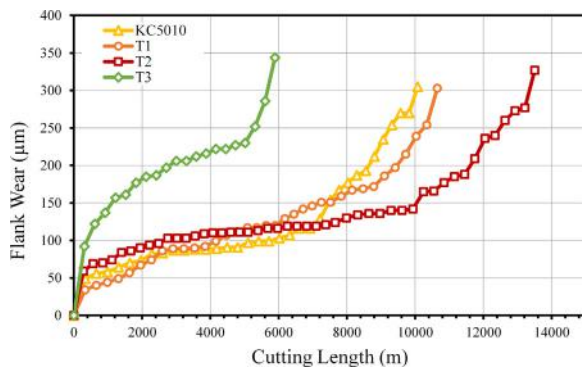
Fig. 4. variation of flank wear versus cutting length for different coatings.
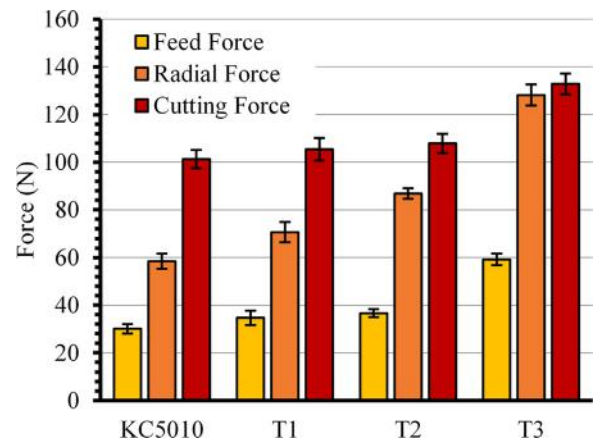
Fig. 5. Variation of cutting forces with coating thickness.

to the rake surface of the tool, since tests are conducted under dry condition [8,14]. However, the significant difference between different coatings lies in the volume of built-up edge formation, which is less extensive in case of the T1–3 coating compared to the benchmark. As the sticking material or built-up edge breaks during the cutting process, it also removes some of the coating/tool material, in other words stick and slip followed by plucking action takes place. By increasing the thickness, the coating can sustain more damage and therefore reduce

the volume of wear. Consequently, the T2 coating demonstrated the least volume of wear (Fig. 7).

To better understand BUE formation, SEM-EDS mapping was performed on the cutting edge at a steady state of wear and a 5000 m length of cut. The results in Fig. 8 show adhesive wear and CGI
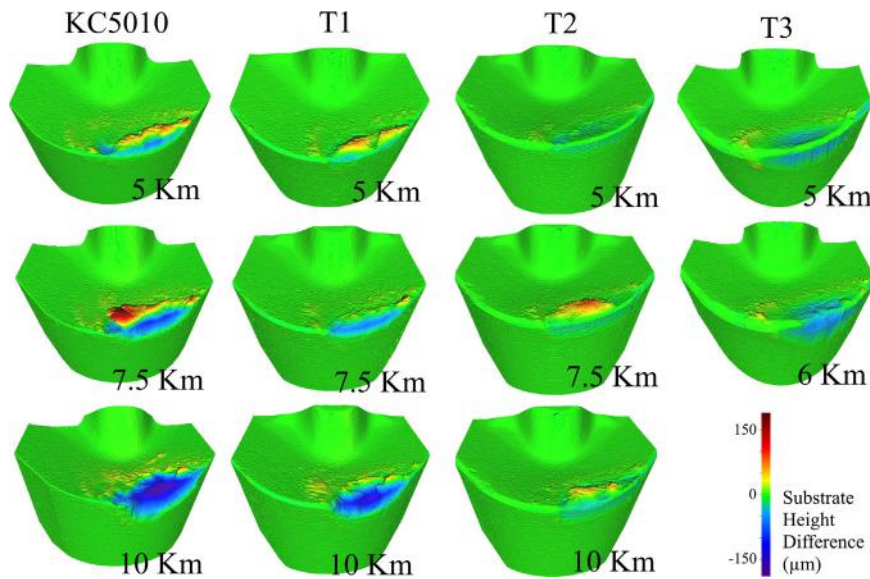
Fig. 6. 3D difference measurement using white light interferometry during the cutting process at 5000, 7500 and 10,000 m length of cut.
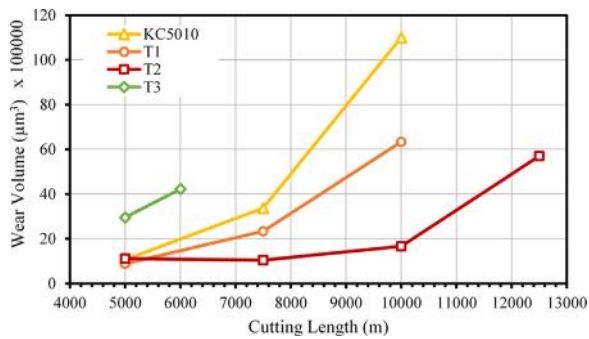
Fig. 7. Volumetric wear of inserts measured by white light interferometry during the cutting process.

adhesion. Therefore, the formation of built-up edge on the rake face is followed by typical abrasive marks on the flank face of the tool. The built-up edge seems to mainly form in the T1 and benchmark coating, since almost little to none BUE is present on the tools coated with T2 and T3. Thus, coatings deposited with the SFC technology (T1–3) could reduce formation of BUE compared to the benchmark, since even the T1 coating showed less BUE at an early stage of wear in Fig. 9. Strong built-up edge formation leads to intensive damage of the surface layer of the coating and results in greater tool wear as can be seen in Fig. 6. A lesser BUE formation probability can be correlated to lower residual stress of the T1–3 coatings. The coating deposited with SFC technology has a higher probability of cohesive failure and crack propagation would require less energy as can be seen from the critical load required for crack initiation in the scratch test (Lc_1 in Fig. 2(c)). Due to the multi-layer nature of the coating, after the cracks are produced, they do not penetrate into the coating, but become deflected within the layers. Therefore, when BUE forms on coatings with low residual stress, it is readily removed by cohesive failure of the coating taking a very small portion of the coating with itself and thus preventing catastrophic failure from happening. However, in case of the benchmark coating, since the coating possesses high resistance to cohesive failure, the BUE grows until cohesive or even adhesive failure occurs. In this manner, SFC deposited coatings (T1-T3) are capable of sustaining operation even under partial flaking of the coating.

FIB/TEM cross-section of the benchmark and T2 coating on the rake face after 400 m of cutting length in Fig. 10(a) and (b) confirms this hypothesis. In case of Fig. 10(a), the benchmark coating is worn out and

the WC-Co substrate is exposed which could be a result of either adhesive failure in the interface or cohesive failure in the substrate. Cohesive failure in the substrate is due to stress distribution in the coating/substrate system and presence of tensile residual stress as Denkena and Breidenstein discussed [30]. On the other hand, the TiAlN SFC multilayer coating can sustain greater adhesive damage. Layer by layer, gradual wear of the coating occurs, along with cohesive failure and partial flaking of the coating. SEM images of the rake face after removing the BUE with $HCl + HNO_3$ in Fig. 10(c) and (d) clearly show substrate exposure of the benchmark tool after a short length of cut (400 m), proving that partial flaking of the T2 coating is taking place on the rake face, which protects the tool from adhesion damage.

3.2.2. Chip undersurface and workpiece surface integrity

SEM images of the chip undersurface collected from the early machining stage of benchmark and T2 coatings are shown in Fig. 11(a) and (b). It was observed that in general, chips have a smoother surface when machining with the T2 coating compared to the benchmark. To confirm this observation, surface roughness values of the chip undersurface were measured using an Lc value of 800 μm. The average value of 10 measurements on different chips showed a surface roughness (S_a) of 1.722 ± 0.254 μm upon machining with the benchmark, and 1.024 ± 0.245 μm upon machining with the T2 coating. Chip undersurface morphology is an excellent indicator of the processes developing at the tool/chip interface. During machining with built-up edge formation, intensive stick-slip phenomena are taking place, which is an indication of catastrophic wear mode. This wear mode leads to severe damage of the friction surface once the built-up edge is broken off. This is confirmed by 3D difference measurement in Fig. 6. While built-up edge formation is impossible to entirely eliminate, it is possible to control this process by decreasing the volume of the built-ups. An efficient way to accomplish this is by adaptive response of the coated cutting tool, particularly by the partial flaking of the coating layer as was shown in the previous section. With strong built-up edge formation, the sticking is stronger (benchmark coating). Because CGI contains a substantial amount of cementite, the sticking phase of the tool/chip interaction leads to detachment of small portions of the workpiece material on the undersurface of the chips (Fig. 11). This results in higher roughness of the chip undersurface. If the size of the built-up edge is significantly reduced, then sticking intensity is lower. In contrast, the slipping phase of the interaction is enhanced and therefore chip undersurface roughness is lower when machining with the T2
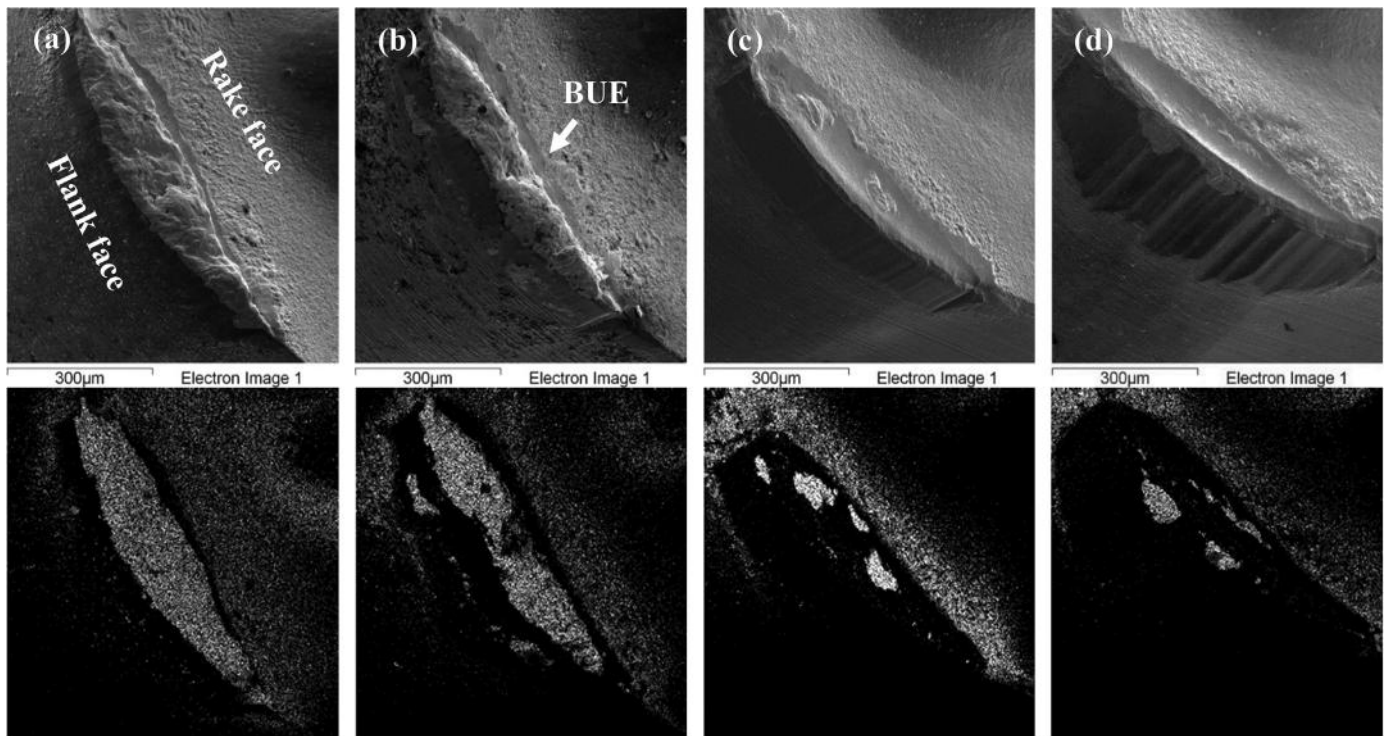
Fig. 8. SEM images and Fe EDS map of the tool with benchmark (a), T1 (b), T2 (c) and T3 (d) coating.
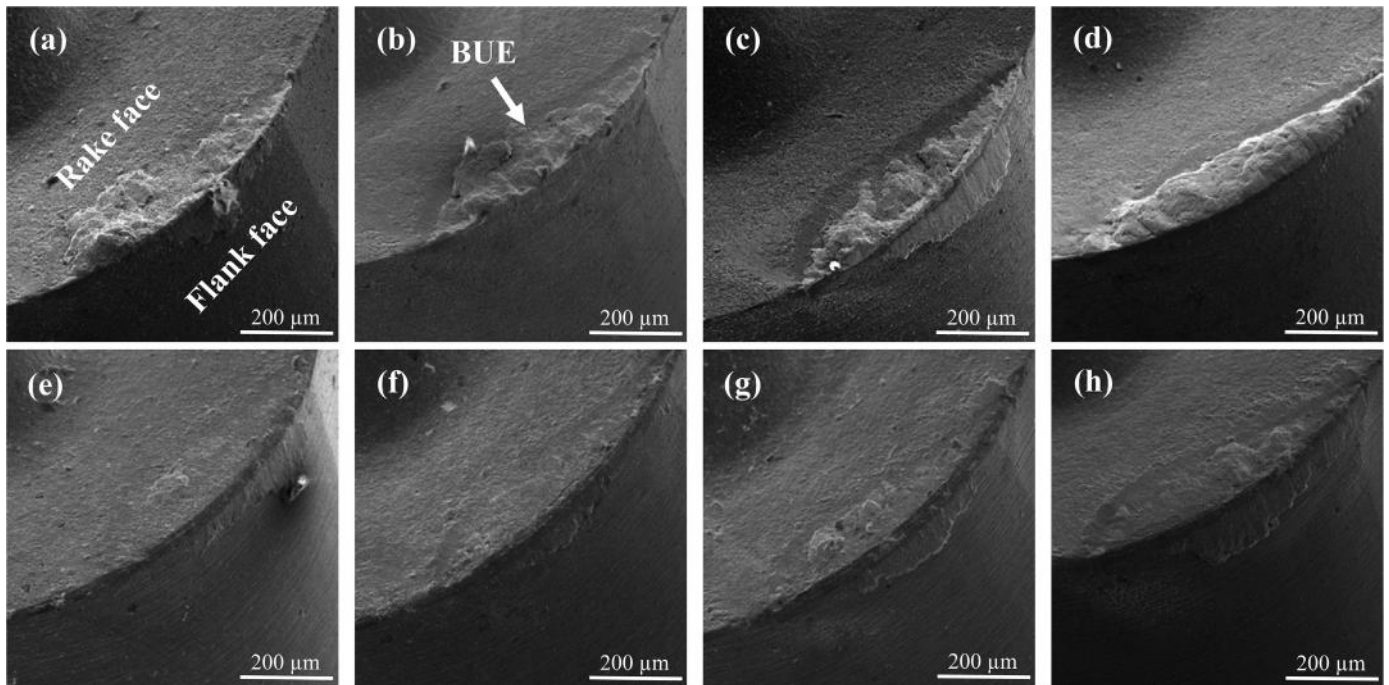
Fig. 9. SEM images of cutting edge with the benchmark (a)-(d) and T1 coating (e)-(h) at 25 m, 75 m, 150 m and 400 m of cutting length.

coating. Cross section of the mentioned chips further proves this fact by showing a greater amount of plastic deformation (higher thickness of secondary shear deformation zone) in the chips collected while machining with the benchmark coating (Fig. 12(a), (b)). A greater degree of plastic deformation is an indication of intensive sticking in the coating/chip interface.

It is also worth mentioning that the surface quality of the machined part also improves under the low residual stress coating (T2) as shown in Fig. 13. Mean value of roughness after 10 measurements on the machined surface shows that the R_a value is 2.507 ± 0.099 μm for the part machined with the benchmark coating, whereas the R_a value is 1.836 ± 0.070 μm for the part machined with the T2 coating. It should be noted that higher edge roundness in the T2 coating (Fig. 1(b)) promotes ploughing, [28] which results in higher Ra values and surface roughness reduction solely as a result of lower BUE formation.
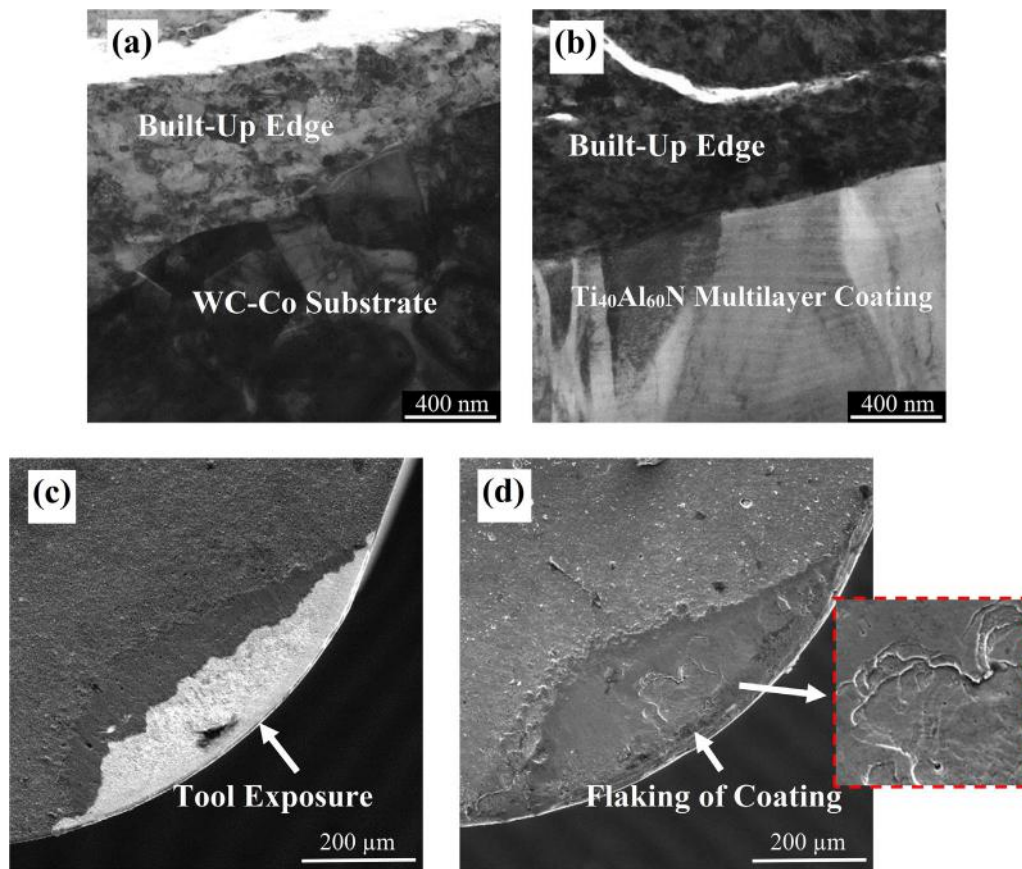
Fig. 10. FIB/SEM cross-section of the rake face of the tool with benchmark (a) and T2 (b) coating and SEM image of rake face after removing BUE of benchmark (c) and T2 (d) coating at 400 m of cutting length.
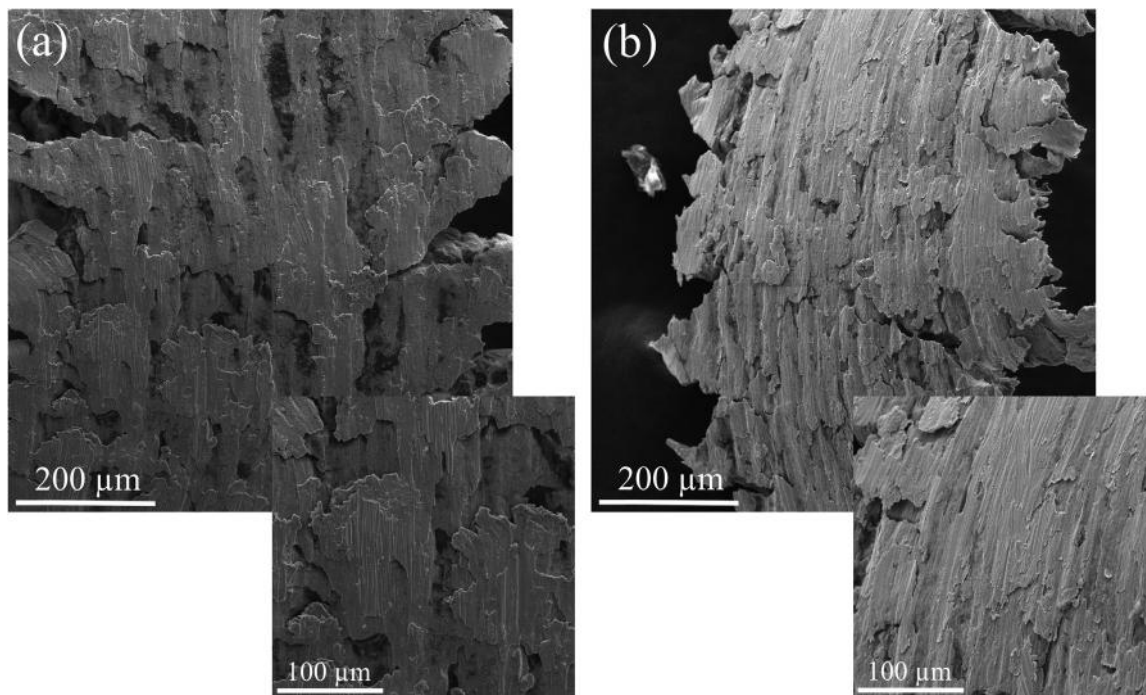
Fig. 11. SEM images of chip undersurface benchmark (a) and T2 (b) coating.
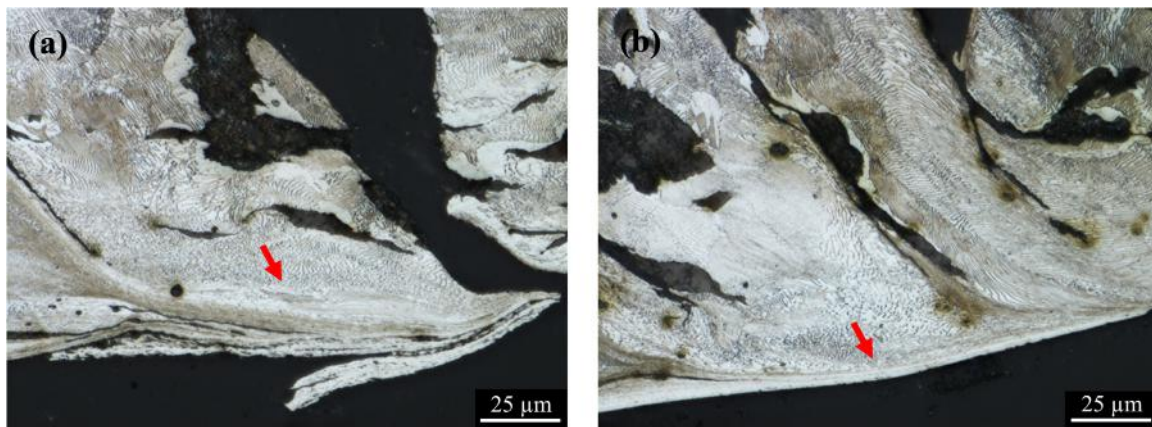
Fig. 12. Chip cross section benchmark (a) and T2 (b) coating.
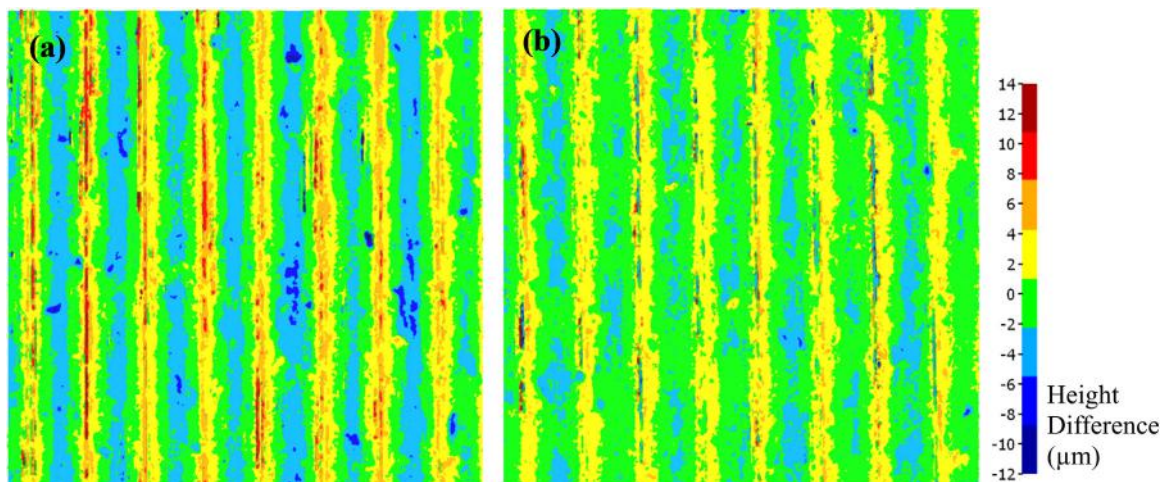
Fig. 13. Height difference measurement of machined surface using benchmark (a) and T2 (b) coating.

4. Conclusion

The effect of PVD coating thickness on tool wear behavior, the mechanical properties of the coating, and the machining performance of CGI turning were presented in this paper. Increasing thickness above a certain value leads to greater rounding of the cutting edge, which promotes higher cutting forces and ploughing, thus inducing an intense wear on the coated tool flank and rake surface in the case study of CGI turning.

Results show that the low residual stress multilayer TiAlN SFC coating succeeds in improving tool life and surface quality of the workpiece by decreasing built-up edge formation and delaying substrate exposure. In fact, three different factors affect the life of tools with increased coating thicknesses:

- First, SFC deposited coatings with low residual stress inhibit BUE formation due to the adaptive response of the coating layer, brought about by the partial superficial flaking of the surface layers of the coating without in-depth crack propagation into the coating layer. This is the major novelty of the obtained results.
- An increasing thickness delays substrate exposure, further increasing the tool life.
- Thickness also influences the microgeometry of the tool, which affects cutting forces as well as thermal and mechanical loads on the coating and can lead to premature failure of the tool if not controlled.

In summary, the combination of these three factors demonstrated an improvement of around 35% in 11 μm thick coatings, which could be considered to be an optimal coating thickness for this specific application.

References

[1] S. Dawson, T. Schroeder, Compacted graphite iron: a viable alternative, Eng. Cast. Solut. AFS (2000).
[2] S. Dawson, T. Schroeder, Practical applications for compacted graphite iron, AFS Trans. C (05) (2004) 1–10.
[3] A. Sahm, E. Abele, H. Schulz, Machining of compacted graphite iron (CGI), Materwiss. Werksttech. 33 (9) (2002) 501–506.
[4] V. Nayyar, J. Kaminski, A. Kinnander, L. Nyborg, An experimental investigation of machinability of graphitic cast iron grades; Flake, compacted and spheroidal graphite iron in continuous machining operations, Procedia CIRP 1 (1) (2012) 488–493.
[5] E. Abele, A. Sahm, H. Schulz, Wear mechanism when machining compacted graphite iron, CIRP Ann. - Manuf. Technol. 51 (1) (2002) 53–56.
[6] M. Gastel, et al., Investigation of the wear mechanism of cubic boron nitride tools used for the machining of compacted graphite iron and grey cast iron, Int. J. Refract. Met. Hard Mater. 18 (6) (2000) 287–296.
[7] M. Heck, H.M. Ortner, S. Flege, U. Reuter, W. Ensinger, Analytical investigations

concerning the wear behaviour of cutting tools used for the machining of com-
pacted graphite iron and grey cast iron, Int. J. Refract. Met. Hard Mater. 26 (3)
(2008) 197–206.

[8] V. Nayyar, G. Grenmyr, J. Kaminski, L. Nyborg, Machinability of compacted gra-
phite iron (CGI) and flake graphite iron (FGI) with coated carbide, Int. J. Mach.
Mach. Mater. 13 (1) (2013) 67.

[9] S. do N. Rosa, A.E. Diniz, C.L.F. Andrade, W.L. Guesser, Analysis of tool wear,
surface roughness and cutting power in the turning process of compact graphite
irons with different titanium content, J. Braz. Soc. Mech. Sci. Eng. 32 (3) (2010)
234–240.

[10] S. Tooptong, K.H. Park, P. Kwon, A comparative investigation on flank wear when
turning three cast irons, Tribol. Int. 120 (2017) (2018) 127–139.

[11] M.B. Da Silva, V.T.G. Naves, J.D.B. De Melo, C.L.F. De Andrade, W.L. Guesser,
Analysis of wear of cemented carbide cutting tools during milling operation of gray
iron and compacted graphite iron, Wear 271 (9–10) (2011) 2426–2432.

[12] A. Malakizadi, et al., Effects of workpiece microstructure, mechanical properties
and machining conditions on tool wear when milling compacted graphite iron,
Wear 410–411 (May) (2018) 190–201.

[13] C. Wang, H. Lin, X. Wang, L. Zheng, W. Xiong, Effect of different oil-on-water
cooling conditions on tool wear in turning of compacted graphite cast iron, J. Clean.
Prod. 148 (2017) 477–489.

[14] G.S. Su, Y.K. Guo, X.L. Song, H. Tao, Effects of high-pressure cutting fluid with
different jetting paths on tool wear in cutting compacted graphite iron, Tribol. Int.
103 (2016) 289–297.

[15] S. Tooptong, K.H. Park, S.W. Lee, P.Y. Kwon, A preliminary machinability study of
flake and compacted graphite irons with multilayer coated and uncoated carbide
inserts, Procedia Manuf. 5 (2016) 644–657.

[16] K.D. Bouzakis, et al., The effect of coating thickness, mechanical strength and
hardness properties on the milling performance of PVD coated cemented carbides
inserts, Surf. Coat. Technol. 177–178 (2004) 657–664.

[17] K.D. Bouzakis, et al., The influence of the coating thickness on its strength prop-
erties and on the milling performance of PVD coated inserts, Surf. Coat. Technol.
174 (175) (2003) 393–401.

[18] G. Skordaris, et al., Film thickness effect on mechanical properties and milling
performance of nano-structured multilayer PVD coated tools, Surf. Coat. Technol.
307 (2016) 452–460.

[19] K. Yamamoto, et al., Cutting performance of low stress thick TiAlN PVD coatings
during machining of compacted graphite cast iron (CGI), Coatings 8 (2) (2018) 38.

[20] K. Tuffy, G. Byrne, D. Dowling, Determination of the optimum TiN coating thick-
ness on WC inserts for machining carbon steels, J. Mater. Process. Technol. 155–156
(1–3) (2004) 1861–1866.

[21] V.G. Sargade, S. Gangopadhyay, S. Paul, A.K. Chattopadhyay, Effect of coating
thickness on the characteristics and dry machining performance of Tin film de-
posited on cemented carbide inserts using cfubms, Mater. Manuf. Process. 26 (8)
(2011) 1028–1033.

[22] F. Klocke, et al., Improved cutting processes with adapted coating systems, CIRP
Ann. - Manuf. Technol. 47 (1) (1998) 65–68.

[23] B.B. He, Introduction to two-dimensional X-ray diffraction, Powder Diffr. 18 (02)
(2003) 71–85.

[24] W. Heinke, A. Leyland, A. Matthews, G. Berg, C. Friedrich, E. Broszeit, Evaluation of
PVD nitride coatings, using impact, scratch and Rockwell- C adhesion tests, Thin
Solid Films 270 (1995) 431–438.

[25] X. Nie, A. Leyland, H.W. Song, A.L. Yerokhin, S.J. Dowey, A. Matthews, Thickness
effects on the mechanical properties of micro-arc discharge oxide coatings on alu-
minium alloys, Surf. Coat. Technol. 116–119 (1999) 1055–1060.

[26] V.K. Sarin, Micro-scratch test for adhesion evaluation of thin films, J. Adhes. Sci.
Technol. 7 (12) (1993) 1265–1278.

[27] S. Zhang, Toughness measurement of thin films: a critical
review (SPEC. ISS), Surf. Coat. Technol. 198 (1–3) (2005) 74–84.

[28] B. Denkena, D. Biermann, Cutting edge geometries, CIRP Ann. - Manuf. Technol. 63
(2) (2014) 631–653.

[29] B. Denkena, B. Breidenstein, Influence of the residual stress state on cohesive da-
mage of PVD-coated carbide cutting tools, Adv. Eng. Mater. 10 (7) (2008) 613–616.

[30] B. Denkena, B. Breidenstein, Residual stress distribution in PVD-coated carbide
cutting tools - origin of cohesive damage, Tribol. Ind. 34 (3) (2012) 158–165.